OXFORD

SOT | Society of Toxicology

www.toxsci.oxfordjournals.org

TOXICOLOGICAL SCIENCES, 149(1), 2016, 237–250

doi: 10.1093/toxsci/kfv231

Advance Access Publication Date: October 26, 2015

Research Article

Inhibition of Human Hepatic Bile Acid Transporters by Tolvaptan and Metabolites: Contributing Factors to Drug-Induced Liver Injury?

Jason R. Slizgi*,[1], Yang Lu*,[1], Kenneth R. Brouwer†, Robert L. St. Claire†, Kimberly M. Freeman†, Maxwell Pan‡, William J. Brock‡,[3], Kim L. R. Brouwer*,[2]

*Division of Pharmacotherapy and Experimental Therapeutics, UNC Eshelman School of Pharmacy, University of North Carolina at Chapel Hill, Chapel Hill, North Carolina 27599; †Qualyst Transporter Solutions, Durham, North Carolina 27713; and ‡Otsuka Pharmaceutical Development and Commercialization, Inc., Rockville, Maryland 20850

[1]These authors contributed equally to this study.

[2]To whom correspondence should be addressed at Division of Pharmacotherapy and Experimental Therapeutics, UNC Eshelman School of Pharmacy, University of North Carolina at Chapel Hill, 301 Pharmacy Lane, CB #7569 Kerr Hall, Chapel Hill, NC 27599-7569. E-mail: kbrouwer@unc.edu

[3]Present address: Brock Scientific Consulting, LLC, Montgomery Village, Maryland 20886

ABSTRACT

Tolvaptan is a vasopressin V_2-receptor antagonist that has shown promise in treating Autosomal Dominant Polycystic Kidney Disease (ADPKD). Tolvaptan was, however, associated with liver injury in some ADPKD patients. Inhibition of bile acid transporters may be contributing factors to drug-induced liver injury. In this study, the ability of tolvaptan and two metabolites, DM-4103 and DM-4107, to inhibit human hepatic transporters (NTCP, BSEP, MRP2, MRP3, and MRP4) and bile acid transport in sandwich-cultured human hepatocytes (SCHH) was explored. IC_{50} values were determined for tolvaptan, DM-4103 and DM-4107 inhibition of NTCP (~41.5, 16.3, and 95.6 μM, respectively), BSEP (31.6, 4.15, and 119 μM, respectively), MRP2 (>50, ~51.0, and >200 μM, respectively), MRP3 (>50, ~44.6, and 61.2 μM, respectively), and MRP4 (>50, 4.26, and 37.9 μM, respectively). At the therapeutic dose of tolvaptan (90 mg), DM-4103 exhibited a C_{max}/IC_{50} value >0.1 for NTCP, BSEP, MRP2, MRP3, and MRP4. Tolvaptan accumulation in SCHH was extensive and not sodium-dependent; intracellular concentrations were ~500 μM after a 10-min incubation duration with tolvaptan (15 μM). The biliary clearance of taurocholic acid (TCA) decreased by 43% when SCHH were co-incubated with tolvaptan (15 μM) and TCA (2.5 μM). When tolvaptan (15 μM) was co-incubated with 2.5 μM of chenodeoxycholic acid, taurochenodeoxycholic acid, or glycochenodeoxycholic acid in separate studies, the cellular accumulation of these bile acids increased by 1.30-, 1.68-, and 2.16-fold, respectively. Based on these data, inhibition of hepatic bile acid transport may be one of the biological mechanisms underlying tolvaptan-associated liver injury in patients with ADPKD.

Key words: drug-induced liver injury; bile acids; hepatic transporters

Autosomal Dominant Polycystic Kidney Disease (ADPKD) is a monogenic inheritable disease characterized by progressive renal cyst development, often leading to end-stage-renal-disease. Supportive care and surgical interventions represent the mainstay of ADPKD treatment because no Food and Drug Administration (FDA)-approved therapy currently exists (Patel *et al.*, 2014; Torres *et al.*, 2007). Tolvaptan, an orally available benzazepine derivative, is a selective vasopressin V_2-receptor antagonist (Yamamura *et al.*, 1998) used in the treatment of clinically significant hyponatremia (Schrier *et al.*, 2006), volume overload in heart failure (Fukunami *et al.*, 2011) and liver cirrhosis with edema (Sakaida, 2014). Tolvaptan recently has shown

promise for delaying renal cyst progression in ADPKD (Boertien *et al.*, 2015; Higashihara *et al.*, 2011; Torres *et al.*, 2012) with approvals in Canada and Europe for this indication. In the pivotal clinical trial, however, tolvaptan was associated with liver injury evident as increased liver enzymes and bilirubin in some patients. No signals of liver injury have been observed in patient populations treated with tolvaptan for other indications or in nonclinical studies (Oi *et al.*, 2011; Watkins *et al.*, 2015). The etiology and/or biological mechanism(s) underlying tolvaptan-associated liver injury in patients with ADPKD have yet to be elucidated.

Drug-induced liver injury (DILI) is a frequent safety concern during drug development that has led to prescribing restrictions for some drugs (eg, trovafloxacin) and market withdrawal for others (eg, troglitazone) (Senior, 2014). Cholestatic and hepatocellular liver injury are 2 major forms of DILI, but despite extensive research, the underlying pathophysiological mechanism(s) remain ill-defined and are likely compound-specific. Inhibition of bile acid transport is one mechanism of DILI leading to intracellular accumulation of hydrophobic bile acids that can cause necrotic and/or apoptotic cell death (Marion *et al.*, 2007; Perez and Briz, 2009; Wagner *et al.*, 2009). The major transport proteins responsible for the basolateral uptake and biliary excretion of bile acids in humans are Na^+-taurocholate cotransporting polypeptide (NTCP/*SLC10A1*) and the bile salt export pump (BSEP/*ABCB11*), respectively. Inhibition of BSEP-mediated bile acid transport has been implicated in DILI (Morgan *et al.*, 2010; Woodhead *et al.*, 2014). In addition, multidrug resistance-associated proteins 2, 3, and 4 (MRP2/*ABCC2*, MRP3/*ABCC3*, and MRP4/*ABCC4*) also transport bile acids and may represent compensatory pathways for hepatic bile acid excretion under duress (Akita *et al.*, 2002; Rius *et al.*, 2006; Zelcer *et al.*, 2003). Recently, our group demonstrated that inhibition of MRP4, in addition to BSEP, may be a risk factor for the development of cholestatic DILI (Köck *et al.*, 2014). Despite the association between bile acid inhibition and DILI, not all bile acid inhibitors cause DILI, suggesting that other mechanism(s) or patient-specific susceptibility factors may play a role in the development of DILI (Morgan *et al.*, 2013).

In humans, tolvaptan exhibits dose-linear pharmacokinetics with an apparent elimination half-life ranging from 3 h to 12 h depending on the dose (Kim *et al.* 2011; Shoaf *et al.* 2007) and an oral bioavailability of ~50% following a 30-mg dose (Shoaf *et al.*, 2012a). Tolvaptan is eliminated primarily by extensive CYP3A metabolism (Shoaf *et al.*, 2012b) with several metabolites detectable in the plasma including an oxybutyric acid metabolite (DM-4103) and a hydroxybutyric acid metabolite (DM-4107) (Figure 1; Sorbera *et al.*, 2002; Tammara *et al.*, 1999). DM-4103 has a long half-life (~180 h) in humans. Following a single, 60-mg oral dose of ^{14}C-tolvaptan, plasma concentrations of DM-4103 are measurable for as long as 456 h and account for ~52% of plasma radioactivity. While circulating concentrations of DM-4107 are lower than tolvaptan (which represents <3% of plasma radioactivity), ~20% of a tolvaptan dose is excreted in urine and feces as this metabolite (Sorbera *et al.*, 2002; Tammara *et al.*, 1999). In addition to the unknown etiology of tolvaptan-associated liver injury in ADPKD patients, it is also unclear whether DILI observed in ADPKD patients is due to the parent compound, a metabolite of tolvaptan, or some other specie(s).

These studies were designed to elucidate the interaction of tolvaptan and 2 metabolites, DM-4103 and DM-4107, with several proteins involved in the hepatic transport of bile acids. In addition, the accumulation and vectorial transport of selected bile acids in the absence and presence of tolvaptan was examined in sandwich-cultured human hepatocytes (SCHH). The results of this investigation, in combination with other ongoing research examining alternative potential mechanisms of hepatotoxicity (eg, mitochondrial toxicity, adaptive immune response), may provide important information to aid in determining the mechanism(s) underlying liver injury in tolvaptan-treated ADPKD patients.

MATERIALS AND METHODS

Materials

[^{3}H]Taurocholic acid (TCA, 15.4 Ci/mmol), [^{3}H]estradiol-17β-glucuronide ($E_2$17G, 41.4 Ci/mmol), and [^{3}H]dehydroepiandrosterone sulfate (DHEAS, 60 Ci/mmol) were purchased from PerkinElmer (Schwerzenbach, Switzerland). Unlabeled substrates (TCA, $E_2$17G, and DHEAS) were purchased from Cayman Chemicals (Ann Arbor, Michigan) or Sigma-Aldrich (St. Louis, Missouri). Stable-labeled TCA (d_8-TCA) and chenodeoxycholic acid (d_5-CDCA) were purchased from Martex Inc. (Minnetonka, Minnesota). Glycochenodeoxycholic acid (GCDCA), taurochenodeoxycholic acid (TCDCA), and erythromycin-estolate were purchased from Sigma-Aldrich. MK-571 was purchased from Cayman Chemicals. A/E Type glass filters (25 mm) used in membrane vesicle studies were purchased from Pall Life Sciences (Ann Arbor, Michigan). Supplements added to culture NTCP-CHO cells were purchased from Invitrogen (Zug, Switzerland). Tolvaptan, DM-4103, and DM-4107 were provided by Otsuka Pharmaceutical Co. Ltd (Tokyo, Japan). The purity of these compounds was >99%.

Cell Culture

Chinese hamster ovary (CHO) cells. CHO cells expressing human NTCP seeded in a 96-well format were obtained from Solvo Biotechnology (Szeged, Hungary). Cells were stored in a humidity-controlled incubator (37°C, 5% CO_2) until used. If possible, studies were completed on the day CHO cells arrived. In the event that experiments were not conducted on the arrival day, the media was replaced according to the supplier's protocol and the experiment was conducted within 24 h.

Sandwich-cultured human hepatocytes. SCHH were prepared by Qualyst Transporter Solutions (Durham, North Carolina) using Transporter Certified cryopreserved human hepatocytes from donor S-1099 (Kaly-Cell, Plobsheim, France) or donor HUM4059 (Triangle Research Laboratories, Durham, North Carolina). Cryopreserved hepatocytes were thawed following the supplier's thawing instructions. SCHH were prepared by plating hepatocytes suspended in propriety hepatocyte QualGro Seeding Medium (Qualyst Transporter Solutions) at a density of 0.7×10^6 viable cells/ml onto BioCoat 24-well cell culture plates (BD Biosciences, San Jose, California). Following plating, cells were allowed to attach for 2–4 h, rinsed and fed with warm (37°C) seeding medium. Eighteen to 24 h later, cells were fed and overlaid with the appropriate species-specific proprietary culture medium (Qualyst Transporter Solutions) supplemented with the extracellular matrix Matrigel (BD Biosciences). Cells were maintained in culture medium in a humidity-controlled incubator (37°C, 5% CO_2) until experiments were conducted on day 5 of culture.

Assays

Membrane vesicle assay. BSEP, MRP2, and MRP4 membrane vesicles were obtained from GenoMembrane (Kanagawa, Japan)

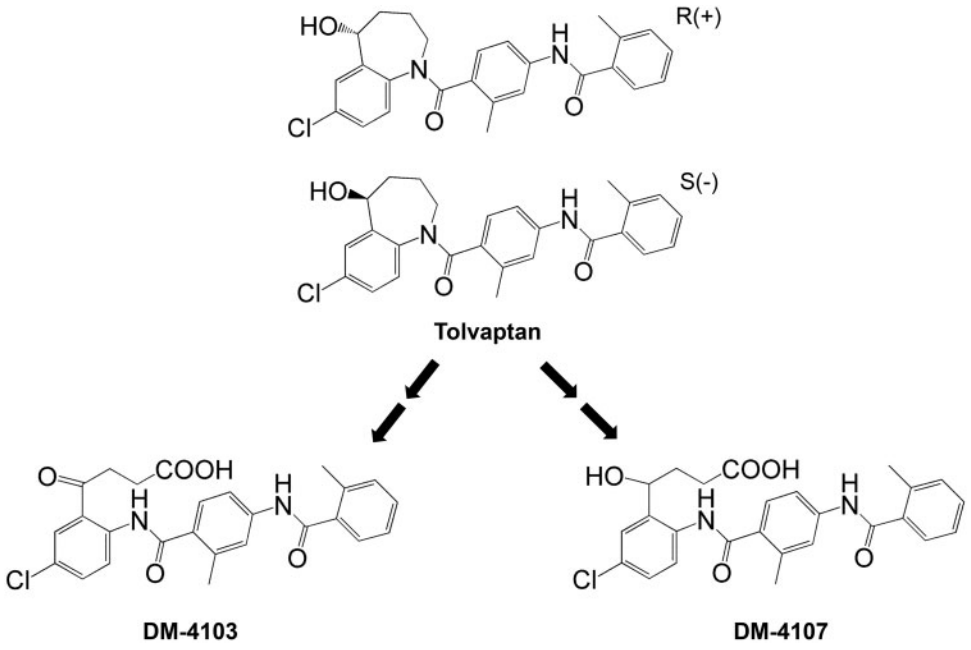

FIG. 1. Chemical structures of tolvaptan, DM-4103, and DM-4107.

and MRP3 membrane vesicles were obtained from Solvo Biotechnology. Membrane vesicles (10 μg BSEP, 5 μg MRP2, 10 μg MRP3, 5 μg MRP4, or control vesicles) were incubated at 37°C with the substrate [^{3}H]TCA, [^{3}H]$E_2$17G, or [^{3}H]DHEAS (2 μCi/ml) supplemented with the unlabeled substrate to achieve a concentration of 2 μM TCA (for BSEP), 50 μM $E_2$17G (for MRP2), 10 μM $E_2$17G (for MRP3), or 2 μM DHEAS (for MRP4) in transport buffer (10 mM Hepes-Tris for BSEP; 40 mM MOPS-Tris for MRP2 and MRP4; 10 mM Tris-HCl for MRP3) containing $MgCl_2$ (10 mM), sucrose (50 mM for BSEP or 250 mM for MRP3) and adenosine triphosphate (ATP) or adenosine monophosphate (AMP) (4 mM) in a final volume of 50 μl. Dimethyl sulfoxide (DMSO) was used to solubilize tolvaptan, DM-4103, and DM-4107; the final concentration of DMSO was <1% vol/vol. After incubation for 2 min (for BSEP and MRP4), 3 min (for MRP2), or 5 min (for MRP3) with vehicle or increasing concentrations of tolvaptan, DM-4103, or DM-4107, the reaction was stopped by the addition of 800 μl ice-cold transport buffer and immediately filtered using A/E glass fiber filters presoaked in transport buffer overnight. The tested concentrations and incubation time points were determined by the limit of solubility for each compound and from preliminary data (data not shown). For the BSEP uptake studies, the filters were presoaked with 1 mM TCA solution to minimize nonspecific binding. For the MRP2, MRP3, and MRP4 uptake studies, the filters were presoaked with 3 mM reduced glutathione and 10 mM dithiothreitol solution to minimize nonspecific binding. The filters were washed 3 times with ice-cold transport buffer using a vacuum filtration system. The filters were transferred to glass vials, and 10 ml liquid scintillation cocktail was added and mixed by vortex before analysis using the Tri-Carb 3100 TR liquid scintillation analyzer (PerkinElmer, Waltham, Massachusetts). The ATP-dependent uptake of substrate was calculated by subtracting substrate uptake in the presence of AMP from substrate uptake in the presence of ATP. The assays were performed in triplicate in 3 separate experiments.

CHO transport studies. CHO cells were rinsed twice with 100 μl of prewarmed (37°C) Krebs-Henseleit uptake buffer with or without Na^+. A third aliquot of 100 μl transport buffer was left on the cells and incubated at 37°C for 15 min. The media was then aspirated and discarded. Uptake was initiated by the addition of prewarmed (37°C) uptake buffer containing the substrate [^{3}H]TCA (2 μCi/ml) supplemented with unlabeled TCA to achieve a concentration of 1 μM. Increasing concentrations of tolvaptan (0–50 μM), DM-4103 (0–75 μM), and DM-4107 (0–200 μM) were added to the substrate solution; the highest concentrations approached the limit of solubility for each compound. DMSO was used to solubilize tolvaptan, DM-4103, and DM-4107; the final concentration of DMSO was <1% vol/vol. The cells were incubated for 5 min at 37°C. Transport was stopped by quick aspiration of the radiolabeled solution; the cells were rinsed 3 times with 100 μl of ice-cold uptake buffer to stop the reaction. The cells were solubilized by adding 100 μL of 100 mM NaOH and left at room temperature for 2 min; 80 μl of the cell suspension was mixed with 5 ml scintillation fluid for radioactivity counting using the Tri-Carb 3100 TR liquid scintillation analyzer (PerkinElmer). NTCP-mediated uptake of TCA was calculated by subtracting substrate uptake in the absence of sodium from substrate uptake in the presence of sodium. The assays were performed in 3 separate experiments in triplicate.

SCHH Studies

Time-, temperature-, and Na^+-dependent uptake of tolvaptan in SCHH. On day 5 of culture, media was aspirated and the SCHH were rinsed with 0.5 ml/well of standard or Ca^{2+}-free Hank's balanced salt solution (HBSS). For Na^+-dependent uptake studies, Na^+-containing or Na^+-free (choline) HBSS buffers were used instead. After the second rinse, HBSS buffers were aspirated completely and SCHH were incubated with 0.5 ml of standard or Ca^{2+}-free HBSS buffers for 10 min (or Na^+-containing or Na^+-free HBSS buffers for the NTCP-mediated uptake studies). After 10 min, HBSS buffers were aspirated and then incubated with standard HBSS buffer containing tolvaptan (15 μM) at 37°C for 5, 10, or 20 min, or 4°C for 10 min. DMSO was used to solubilize tolvaptan; the final concentration of DMSO was 0.2% vol/vol. For the Na^+-dependent uptake studies,

tolvaptan was incubated at 37°C for 10 min. A tolvaptan concentration of 15 μM was selected because it was the highest concentration in the linear range for tolvaptan uptake (data not shown). After incubation, the HBSS buffer was aspirated from all wells and rinsed 3 times with ice-cold standard HBSS buffer. Plates were sealed and stored at −80°C until analysis.

Hepatobiliary disposition of TCA, CDCA, TCDCA, and GCDCA in the presence of tolvaptan. On day 7 of culture, culture media was aspirated completely and SCHH were rinsed with 0.5 ml/well of standard or Ca^{2+}-free HBSS buffers. After the second rinse, HBSS buffers were aspirated completely and SCHH were incubated with 0.5 ml of standard or Ca^{2+}-free HBSS buffers for 10 min. After 10 min, HBSS buffers were aspirated completely and then incubated with the standard HBSS containing 2.5 μM of the probe substrate (d_8-TCA, d_5-CDCA, TCDCA, or GCDCA) with or without tolvaptan (15 μM) for 10 min. After incubation, the incubation solutions were aspirated from all wells and rinsed 3 times with ice-cold standard HBSS buffer. Plates were sealed and stored at −80°C until analysis.

Analysis of tolvaptan, DM-4103, and DM-4107 in SCHH and media by liquid chromatography-tandem mass spectrometry (LC-MS/MS). A volume of 500 μl of lysis solution [70:30 methanol:water (v:v) containing 27.5 nM internal standard] was added to each well of previously frozen 24-well plates containing study samples. Plates were shaken for ∼15 min and the cell lysate solution was transferred to a Whatman 96-well Unifilter 25 μm MBPP/0.45 μm PP filter plate (Maidstone, England) stacked on a 96-well deepwell plate. Lysate was filtered into the deepwell plate by centrifugation (2000 × g for 5 min). The sample filtrate was evaporated to dryness and the samples were reconstituted in 200 μl sample diluent (70:30 methanol:water containing 0.1% formic acid) and mixed for 15 min on a plate shaker. The reconstituted samples were transferred to a 0.45-μm filter plate (Millipore, Billerica, Massachusetts) and filtered into a 96-well plate by centrifugation (2000 × g for 2 min) and sealed with a silicone capmat prior to LC-MS/MS analysis. Analytical controls for tolvaptan, DM-4103, and DM-4107 were measured using standard curves. Analytical standards were prepared over a range of concentrations to deliver, with the addition of a 10-μl volume per well, the range of mass 0.5–5000 pmoles/well for tolvaptan, DM-4103, and DM-4107. Cell lysates from SCHH were utilized for the generation of standard curves and related quality control (QC) samples. QC lysate samples were prepared at the lower limit of quantitation (LLQ) and the upper limit of quantitation (ULQ). These lysate controls were further processed as described above. A binary HPLC system (Shimadzu, Columbia, Maryland) composed of LC-10ADvp pumps, a CTO-10Avp oven, and an HTC-96-well autosampler was used. The chromatographic column was a Hypersil Gold C18 (100 × 1.0 mm^2, 3 μm) with matching guard (5 μm) and pre-column filter (Thermo Scientific, Bellefont, Pennsylvania). Column temperature was maintained at 35°C. A mobile phase gradient composed of A = 50% methanol with 0.1% formic acid and B = 90% methanol with 0.01% formic acid was used at a flow rate of 50 μl/min and a total run time of 10 min. All test compounds were chromatographically resolved. The gradient profile was: initial 25% B for 2.0 min; from 2.0 to 5.0 min ramp to 100% B and hold for 0.9 min; step back to 25% B at 6.0 min and re-equilibrate for 4.0 min. An injection volume of 5 μl was used. Tandem mass spectrometry with positive ion electrospray ionization was conducted with a Thermo Electron TSQ Quantum Discovery MAX (Thermo Fisher, Waltham, Massachusetts) with an Ion Max ESI source. The transitions monitored (parent *m/z* > product *m/z*) at unit resolution for tolvaptan, the internal standard, DM-4103, and DM-4107 were 449.2 > 252.0, 463.2 > 266.0, 479.0 > 252.0, and 481.0 > 252.0, respectively. The analytical run was typically conducted with a standard curve at the beginning of the run. A ULQ QC and a LLQ QC sample were placed in the middle of the run and at the end of the run. Analyte and internal standard peak area responses were determined for the standards, QC's, and unknown samples, and the unknown and QC samples (pmoles/well) were calculated utilizing the standard curve. Analytical run ruggedness was evaluated based on percent accuracy of the back calculated values for the standards and QC's. Acceptance criteria for percent accuracy of back calculated values were typically 15%–20%.

Analysis of TCA, CDCA, TCDCA, and GCDCA. Analysis of d_8-TCA, d_5-CDCA, TCDCA, and GCDCA was performed using LC-MS/MS as described previously (Marion *et al.*, 2012). Assay acceptance criteria were similar to those defined above. For the analysis of TCDCA and GCDCA only, the relative amounts (no standard curve) were determined by measuring the peak area ratios from the unknown LC-MS/MS peak area and the area of the corresponding internal standard. Relative changes were determined for individual treatments.

Data Analysis and Statistics

Membrane vesicle and CHO cell assays. Transporter-mediated uptake was normalized to vehicle control values (without inhibitor). IC_{50} values were determined by nonlinear regression techniques using the following equation in GraphPad Prism 6 (San Diego, California):

$$Y = 100/\left[1 + 10^{\left(X - \mathrm{LogIC}_{50}\right)}\right],$$

where *X* represents the log concentration of inhibitor and *Y* represents the percentage of control activity. Data are reported as the point estimate and 95% confidence interval (CI). If the inhibitor did not reduce substrate transport by >50% at the highest tested concentration, nonlinear regression to estimate an IC_{50} value was not conducted. The type of inhibition and inhibition constant (K_i) for BSEP-mediated TCA transporter was determined by fitting competitive, noncompetitive, and uncompetitive models to the untransformed data by nonlinear regression analysis using GraphPad Prism 6. The best-fit model was assessed based on visual inspection of the observed versus predicted data and the Akaike Information Criteria (Akaike, 1974). Equations used for each inhibition model were as follows:

$$\text{Competitive}: \nu = \frac{V_{max} \times S}{K_m \times \left(1 + \frac{I}{K_i}\right) + S}$$

$$\text{Noncompetitive}: \nu = \frac{V_{max} \times S}{K_m \times \left(1 + \frac{I}{K_i}\right) + S \times \left(1 + \frac{I}{K_i}\right)}$$

$$\text{Uncompetitive}: \nu = \frac{V_{max} \times S}{K_m + S \times \left(1 + \frac{I}{K_i}\right)},$$

where *S* represents the concentration of TCA, *I* represents the concentration of tolvaptan or DM-4103, ν represents the rate of TCA transport, V_{max} represents the maximal rate of TCA transport, K_m represents the TCA concentration that yields one-half

maximal TCA transport, and K_i represents the dissociation constant for the BSEP-inhibitor complex. Data are from $n = 3$ independent experiments in triplicate.

Sandwich-cultured hepatocyte studies. All mass values were normalized to the mean protein (mg) content per well from SCHH. Protein content was determined using the Pierce BCA protein assay kit. Cellular accumulation determined in Ca^{2+}-free HBSS buffer was assumed to represent the total mass of analyte inside the hepatocyte at the end of the incubation time period. Total accumulation determined in standard HBSS buffer represents the total mass of compound taken up and excreted (cells + bile). The biliary excretion index (BEI) was calculated according to the following equation (Liu *et al.*, 1999a):

$$\mathrm{BEI}(\%) = \frac{\mathrm{Accumulation}_{\text{Standard HBSS}} - \mathrm{Accumulation}_{\text{Ca}^{2+}\text{-free HBSS}}}{\mathrm{Accumulation}_{\text{Standard HBSS}}} \times 100$$

The *in vitro* biliary clearance ($Cl_{biliary}$) was determined using the following equation (Ghibellini *et al.* 2007; Liu *et al.*, 1999b) and was scaled to body weight using scaling factors (Qualyst Transporter Solutions Technical Application Bulletin, 2011).

$$Cl_{biliary} = \frac{\mathrm{Accumulation}_{\text{Standard HBSS}} - \mathrm{Accumulation}_{\text{Ca}^{2+}\text{-free HBSS}}}{\text{time} \times \text{concentration}_{\text{media}}}$$

The biliary clearance for DM-4103 and DM-4107 could not be determined because the metabolites were generated endogenously. The intracellular concentration of each test compound was calculated by dividing the mass of compound in cells by the respective hepatocyte intracellular fluid volume for human hepatocytes (7.69 µl/mg protein; Qualyst Transporter Solutions Technical Application Bulletin, 2011). All calculations were performed using Microsoft Excel (Redmond, Washington).

RESULTS

NTCP- and BSEP-Mediated TCA Transport

TCA was used as a substrate to study the interaction of tolvaptan, DM-4103, and DM-4107 with the basolateral uptake transporter NTCP. TCDCA (100 µM) was used as a positive control and inhibited NTCP-mediated uptake by >98% (data not shown). The estimated IC_{50} values for tolvaptan, DM-4103, and DM-4107 were ~41.5, 16.3, and 95.6 µM, respectively (Figs. 2A–C; Table 1). TCA was used as a substrate to study the interaction of tolvaptan, DM-4103, and DM-4107 with the canalicular efflux transporter BSEP. Rifampicin (50 µM) was used as a positive control and inhibited BSEP-mediated uptake by >50% (data not shown; Byrne *et al.*, 2002). BSEP-mediated TCA uptake was reduced to 16.4% of control when incubated with 50 µM tolvaptan; the estimated IC_{50} value was 31.6 µM (Figure 2D; Table 1). DM-4103 inhibited BSEP-mediated TCA uptake with an IC_{50} value of 4.15 µM, while the IC_{50} value for DM-4107 was 119 µM (Figs. 2E

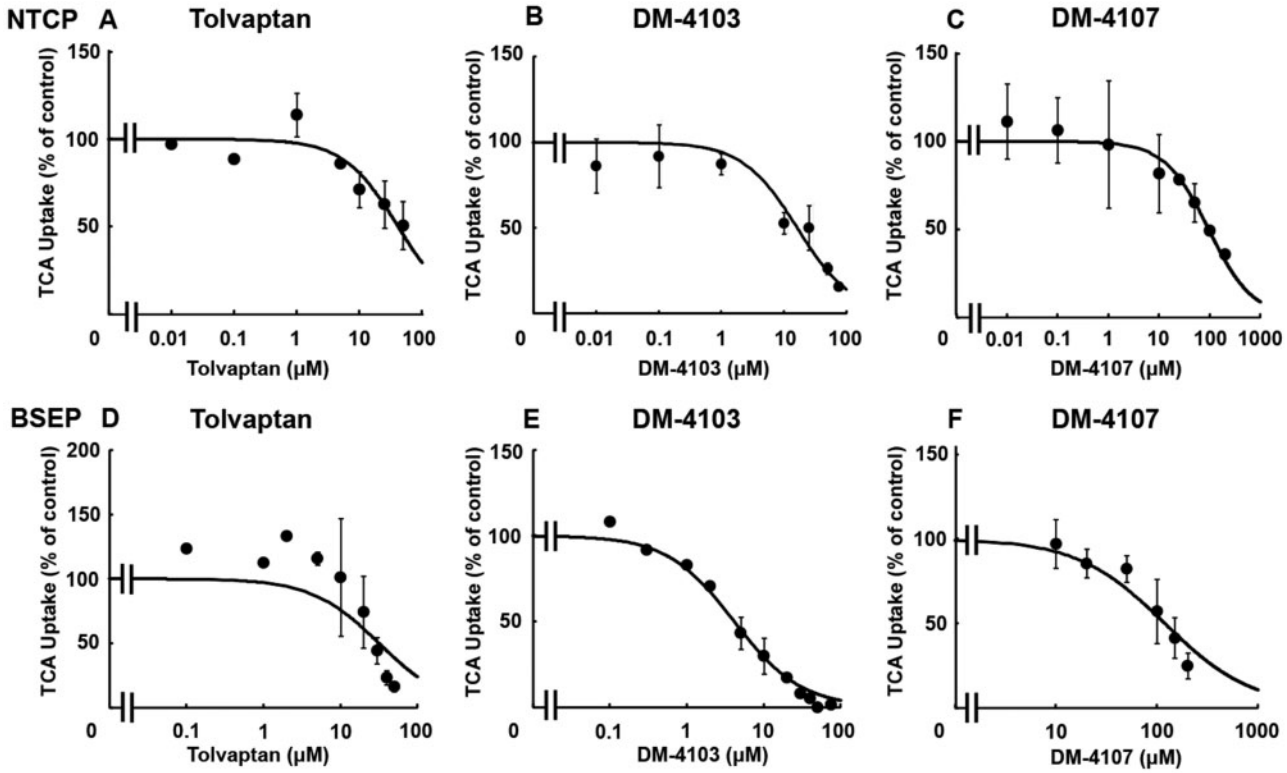

FIG. 2. Effect of tolvaptan, DM-4103, and DM-4107 on NTCP-mediated transport or BSEP-mediated transport of TCA. NTCP-overexpressing cells were co-incubated with tolvaptan (0–50 µM), DM-4103 (0–75 µM), or DM4107 (0–200 µM) and [^{3}H]TCA (2 µCi/ml; 1 µM) for 5 min at 37°C (A-C); BSEP vesicles were co-incubated with tolvaptan (0–50 µM), DM-4103 (0–75 µM), or DM4107 (0–200 µM) and [^{3}H]TCA (2 µCi/ml; 2 µM) for 2 min at 37°C (D-F). NTCP-mediated uptake of TCA was calculated by subtracting substrate uptake in the absence of sodium from substrate uptake in the presence of sodium. BSEP-mediated transport was calculated by subtracting TCA uptake in the presence of AMP from TCA uptake in the presence of ATP. Values are expressed as percentage of vehicle control; each value represents the mean ± SD from 3 independent experiments. The curve represents the best fit line using nonlinear regression techniques. See "Materials and Methods" section for further details.

and F). The K_i was estimated using nonlinear regression by incubating BSEP membrane vesicles with TCA (2–30 μM) and designated concentrations of tolvaptan (0–50 μM) or DM-4103 (0–20 μM). A K_i for DM-4107 was not determined because it was a less potent inhibitor of BSEP-mediated TCA transport based on the estimated IC_{50} value compared with tolvaptan and DM-4103. Nonlinear regression analysis of the data revealed that tolvaptan was best described by a noncompetitive inhibition model ($K_i = 34.2$ μM), while DM-4103 was best described by a competitive inhibition model ($K_i = 3.77$ μM) (Figure 3).

TABLE 1. Inhibitory Potency of Tolvaptan, DM-4103, and DM-4107 on Transporter-Mediated Uptake

Transporter	Inhibitor	IC_{50} (μM)	95% CI (μM)	C_{max}/IC_{50}
NTCP	Tolvaptan	~41.5	26.0–66.3	0.03
	DM-4103	16.3	11.1–24.0	0.96*
	DM-4107	95.6	58.7–156	0.02
BSEP	Tolvaptan	31.6	16.5–60.3	0.04
	DM-4103	4.15	3.45–4.99	3.78*
	DM-4107	119	86.2–163	0.02
MRP2	Tolvaptan	>50	NC	NC
	DM-4103	~51.0	32.0–81.3	0.31*
	DM-4107	>200	NC	NC
MRP3	Tolvaptan	>50	NC	NC
	DM-4103	~44.6	30.9–64.5	0.35*
	DM-4107	61.2	51.5–72.8	0.04
MRP4	Tolvaptan	>50	NC	NC
	DM-4103	4.26	3.32–5.47	3.69*
	DM-4107	37.9	32.1–44.7	0.06

IC_{50} values were determined by nonlinear regression techniques as described in "Materials and Methods" section; data are reported as the IC_{50} estimate and 95% CI of $n = 3$ independent experiments in triplicate. Mean C_{max} values were determined in subjects following a 90-mg dose of tolvaptan (Watkins *et al.*, 2015).

CI: confidence interval; mean C_{max} following a 90-mg dose in humans; NC: noncalculable. In cases where substrate uptake was inhibited by >50% only at the highest tested inhibitor concentration, the data were curve fit in the usual manner, but the estimated IC_{50} value was designated as an approximation (~). If the inhibitor did not reduce substrate transport by >50% at the highest tested concentration, nonlinear regression to estimate an IC_{50} value was not conducted and the value was reported as greater than the highest tested concentration. *C_{max} values were not determined in clinical trials, therefore, concentrations at steady-state were used instead.

MRP2- and MRP3-Mediated $E_2$17G Transport, and MRP4-Mediated DHEAS Transport

$E_2$17G and DHEAS were used as substrates to study the interaction of tolvaptan, DM-4103, and DM4107 with the efflux transporters MRP2, MRP3, and MRP4. MK-571 (50 μM) was used as a positive control and inhibited MRP2-, MRP3- and MRP4-mediated transport by >95%, >50%, and >90%, respectively (data not shown). If transporter-mediated uptake of a probe substrate was not inhibited by >50%, nonlinear regression analysis was not conducted (Figs. 4C, D, and G). At the highest concentration of tolvaptan, MRP2-mediated $E_2$17G uptake was 115% of control, indicating that tolvaptan did not inhibit MRP2 transport (Figure 4A). The estimated IC_{50} value for DM-4103 was ~51.0 μM (Figure 4B). The estimated IC_{50} values for DM-4103 and DM-4107 mediated MRP3 inhibition were ~44.6 and 61.2 μM, respectively (Figs. 4E and F; Table 1). DHEAS was used as a substrate to study the interaction of tolvaptan, DM-4103 and DM4107 with the basolateral efflux transporter MRP4. At the highest concentration of tolvaptan (50 μM), MRP4-mediated DHEAS uptake was 88% of control, indicating that tolvaptan had minimal impact on MRP4 transport (Figure 4G). The estimated IC_{50} values for DM-4103 and DM-4107 were 4.26 and 37.9 μM, respectively (Figs. 4H and I; Table 1).

DM-4103 inhibited MRP2-mediated $E_2$17G uptake by >50% only at the highest tested concentration (Figure 4B). Although a curve was fit to these data to estimate an IC_{50} of ~51.0 μM, caution must be exercised when interpreting this value. The limits of solubility precluded testing higher concentrations of DM-4103. Such was the case with MRP3-mediated inhibition by DM-4103 as well as NTCP-mediated inhibition by tolvaptan (Figs. 2A and 4E).

Time- and Temperature-Dependent Uptake of Tolvaptan in SCHH

SCHH were incubated with tolvaptan (15 μM) for 5, 10, or 20 min at 37°C or for 10 min at 4°C. Tolvaptan accumulated in SCHH reaching a concentration of ~500 μM after 10 min, assuming that binding to the hepatocyte surface was negligible and that accumulation represented the mass of tolvaptan in the cell. Temperature-dependent uptake suggested that both active and passive components are involved in tolvaptan uptake (Figure 5A). The BEI for tolvaptan was <10%, indicating a low potential for biliary excretion of tolvaptan. In separate SCHH studies, formation of both DM-4103 and DM-4107 was observed during a 10-min incubation with tolvaptan (15 μM) at 37°C (Figure 5B); the mean total (bound + unbound) cellular

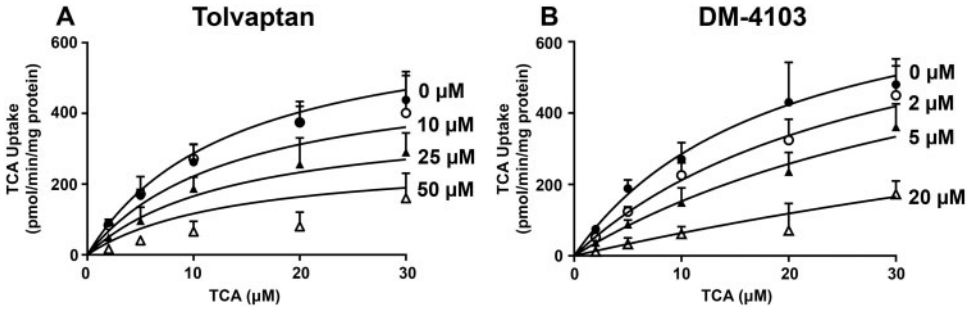

FIG. 3. Effect of tolvaptan and DM-4103 on BSEP-mediated transport of TCA. Uptake of TCA (2, 5, 10, 20, or 30 μM) was determined in the presence of 0 μM (•), 10 μM (○), 25 μM (▲), or 50 μM (Δ) tolvaptan (A) or 0 μM (•), 2 μM(○), 5 μM (▲), or 20 μM (Δ) of DM-4103 (B). TCA uptake was measured after an incubation of 2 min at 37°C in the presence or absence of inhibitor. BSEP-mediated transport was calculated by subtracting TCA uptake in the presence of AMP from TCA uptake in the presence of ATP; each value represents the mean ± SD from 3 independent experiments. The curves represent the best fit model using nonlinear regression techniques. See "Materials and Methods" section for further details.

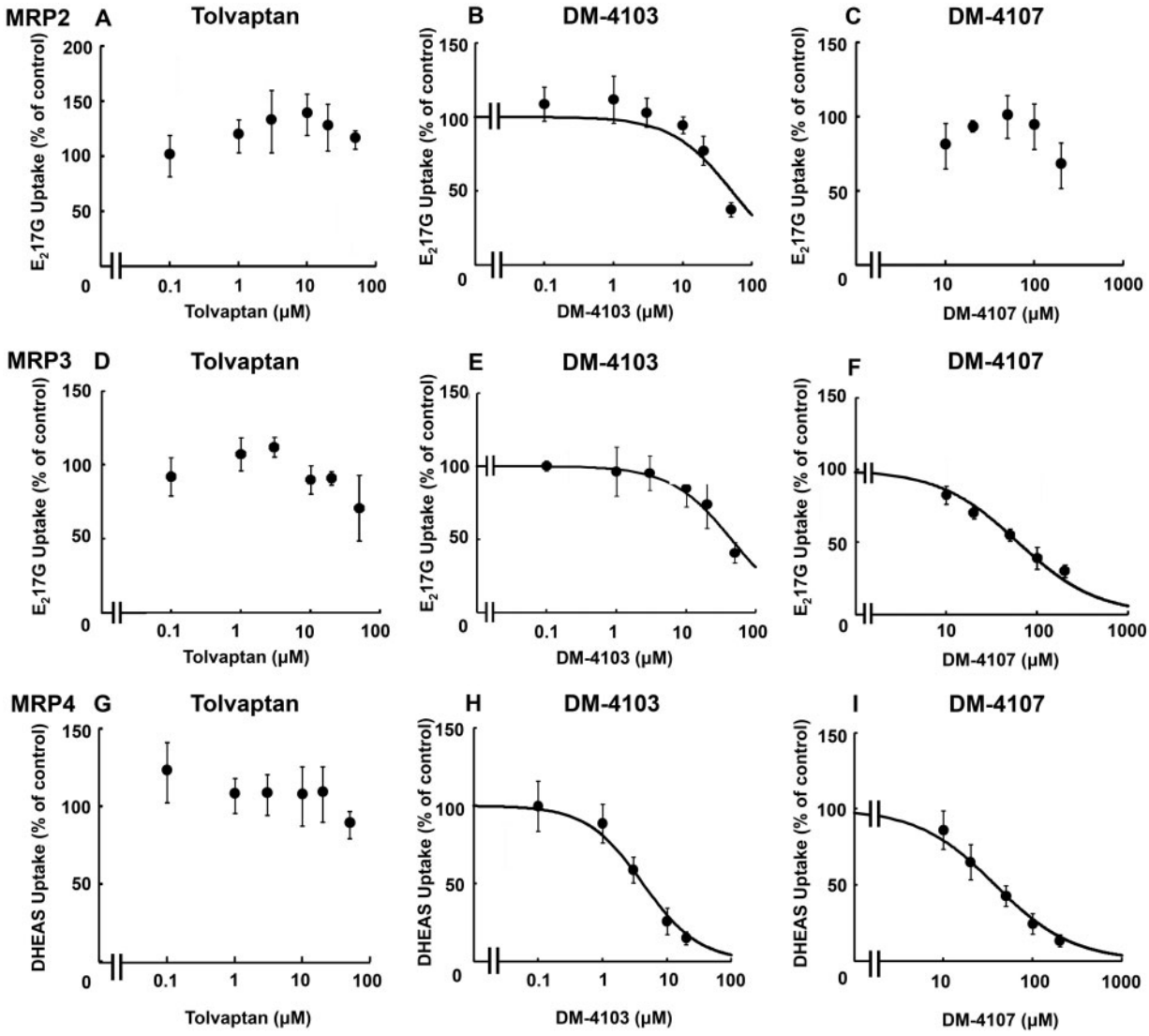

FIG. 4. Effect of tolvaptan, DM-4103, and DM-4107 on MRP2-mediated transport of $E_2$17G, MRP3-mediated transport of $E_2$17G, and MRP4-mediated transport of DHEAS. MRP2 (A–C), MRP3 (D–F), or MRP4 (G–I) vesicles were co-incubated with tolvaptan (0–50 μM), DM-4103 (0–50 μM for MRP2 and MPR3, and 0–20 μM for MRP4), or DM-4107 (0–200 μM) and [^{3}H]$E_2$17G (2 μCi/ml; 50 μM) (A–C) for 2 min, [^{3}H]$E_2$17G (2 μCi/ml; 10 μM) (D–F) for 5 min, or [^{3}H]DHEAS (2 μCi/ml; 2 μM) (G–I) for 2 min at 37°C. MRP-mediated transport was calculated by subtracting substrate uptake in the presence of AMP from substrate uptake in the presence of ATP. Values are expressed as percentage of vehicle control; each value represents the mean ± SD from 3 independent experiments. If the inhibitor did not reduce substrate transport by >50% at the highest tested concentration, nonlinear regression to estimate an IC_{50} value was not conducted. The curve represents the best fit line using nonlinear regression techniques. See "Materials and Methods" section for further details.

concentrations of tolvaptan, DM-4103 and DM-4107 were 530, 1.71, and 35.6 μM, respectively.

Sodium-Dependent (NTCP) Uptake of Tolvaptan in SCHH

To determine the sodium-dependent uptake of tolvaptan in SCHH, hepatocytes were incubated in the presence or absence of sodium. The total accumulation of tolvaptan and the accumulation of generated DM-4103 and DM-4107 were unaffected by the absence of sodium (Table 2).

Hepatobiliary Disposition of TCA, CDCA, TCDCA, and GCDCA in the Presence of Tolvaptan in SCHH

The effect of tolvaptan on the hepatobiliary disposition of 4 model bile acids (TCA, CDCA, TCDCA, and GCDCA) was evaluated in SCHH. When co-incubated with 15 μM tolvaptan, the total accumulation of TCA was decreased by 32.6% and the BEI was decreased by 15.7% compared to control (Table 3). The combined effect of the inhibition of both uptake and efflux by tolvaptan decreased the biliary clearance of TCA by 43% compared to control (Table 3; Figure 6A). In contrast to TCA, the cellular accumulation of CDCA tended to increase by 1.3-fold relative to control. Tolvaptan-mediated changes in the biliary clearance and BEI of CDCA were decreased by 55% and 61%, respectively, compared to control (Table 3). Erythromycin estolate (100 μM), a broad-spectrum efflux transport inhibitor, was used as a positive control and had no effect on the total accumulation (cell + bile) of CDCA, but inhibited the biliary excretion of CDCA (data not shown). Similar to CDCA, tolvaptan had no effect on the total accumulation of TCDCA or GCDCA, but did appear to increase the cellular accumulation (cells) of TCDCA and GCDCA by 1.68- and 2.16-fold, respectively, compared with control when co-incubated with tolvaptan (Table 3; Figure 6B).

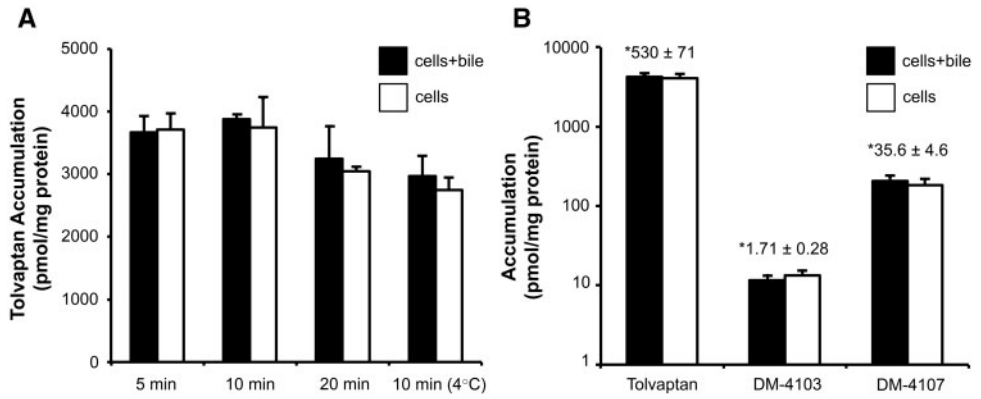

FIG. 5. Time- and temperature-dependent accumulation of tolvaptan in SCHH. Accumulation of tolvaptan in cells + bile (black bars) and cells (white bars) was measured by incubating SCHH with 15 μM of tolvaptan for 5, 10, or 20 min at 37°C, or for 10 min at 4°C (A). Accumulation of tolvaptan, and the generated metabolites DM-4103 and DM-4107 in cells + bile (black bars) and cells (white bars) was measured by incubating SCHH with 15 μM of tolvaptan for 10 min at 37°C (B). *Cellular concentrations were calculated using the total mass of tolvaptan, DM-4103, or DM-4107 in cells (white bars) and hepatocyte fluid volume as described in "Materials and Methods" section; each value represents the mean ± SD from $n = 1$ liver in triplicate.

TABLE 2. Sodium-Dependent Uptake of Tolvaptan, DM-4103 and DM-4107 in SCHH

Tolvaptan dose concentration	Buffer	Tolvaptan Total accumulation (pmol/mg)	DM-4103 Total accumulation (pmol/mg)	DM-4107 Total accumulation (pmol/mg)
15 μM	Sodium	2730 ± 397	7.82 ± 0.84	121 ± 19
	Choline	3460 ± 684	8.35 ± 0.83	136 ± 16

Accumulation of tolvaptan, DM-4103, and DM-4107 was measured by incubating SCHH with 15 μM of tolvaptan for 10 min in the presence or absence of sodium, as described in "Materials and Methods" section. Data are presented as mean ± SD ($n = 1$ liver in triplicate).

TABLE 3. Hepatobiliary Disposition of 2.5 μM TCA, Chenodeoxytaurocholic acid (CDCA), TCDCA or GCDCA in the absence or presence of tolvaptan (15 μM) in SCHH

Probe	Inhibitor	Total accumulation[a]	Cellular accumulation[a]	$Cl_{biliary}$ (ml/min/kg)	BEI (%)
TCA	Vehicle control	215 ± 27	43.3 ± 4.4	20.3	79.8
	Tolvaptan	145 ± 16	47.5 ± 2.1	11.6	67.3
CDCA	Vehicle control	580 ± 67	469 ± 60	13.1	19.1
	Tolvaptan	658 ± 86	608 ± 31	5.86	7.52
TCDCA	Vehicle control	3.37 ± 0.55	0.545 ± 0.049	NC	83.8
	Tolvaptan	3.32 ± 0.27	0.915 ± 0.22	NC	71.0
GCDCA	Vehicle control	8.82 ± 0.98	0.892 ± 0.065	NC	89.2
	Tolvaptan	7.55 ± 1.28	1.93 ± 0.28	NC	74.5

[a]Accumulation of TCA, CDCA, TCDCA, or GCDCA was measured by incubating SCHH with or without 15 μM of tolvaptan for 10 min in standard (total accumulation) or Ca^{2+}-free (cellular accumulation) HBSS, as described in *Materials and Methods*. Data are presented as mean ± SD ($n = 1$ liver in triplicate). Accumulation of TCA and CDCA is expressed as pmol/mg protein; accumulation of TCDCA and GCDCA is expressed as peak area ratio; BEI = biliary excretion index; NC: non-calculable.

DISCUSSION

In this study, the inhibitory effect of tolvaptan, DM-4103, and DM-4107 on human hepatic bile acid transporters was investigated. This study was undertaken because tolvaptan was associated with liver injury in some patients with ADPKD during clinical investigation. Liver injury had not been reported previously for other patient populations, eg, patients treated for hyponatremia, or cardiac and hepatic edema. In the ADPKD pivotal trial and the subsequent ongoing open-label safety study (NCT01214421), 4.9% of patients treated with tolvaptan had elevated alanine aminotransferase levels compared with 1.2% of those receiving the placebo (Torres *et al.*, 2012). Fewer patients treated with tolvaptan than those receiving the placebo (0.9% vs 1.9%) had increased bilirubin levels. However, 2 cases of Hy's Law were observed in tolvaptan-treated ADPKD patients, while no Hy's Law cases were reported in placebo-treated patients (Torres *et al.*, 2012). A third case of Hy's Law was observed in a tolvaptan-treated ADPKD patient in an open-label follow on trial (Watkins *et al.*, 2015). Furthermore, these observations did not appear to be associated with dose or exposure and generally occurred after 3 months or more of treatment (Watkins *et al.*, 2015).

Idiosyncratic DILI is, by definition, a rare event. There was no apparent correlation between renal impairment, apparent hepatorenal cyst burden or stage of ADPKD and occurrence of hepatic events. Because of the low number of events, a definitive conclusion about an association between cyst burden and DILI cannot be made at this time. These data were described at the FDA Advisory Committee meeting for tolvaptan (August 2013; www.fda.gov) but have not been published yet. Interestingly, systemic tolvaptan exposure based on AUC was greater in patients with reduced creatinine clearance

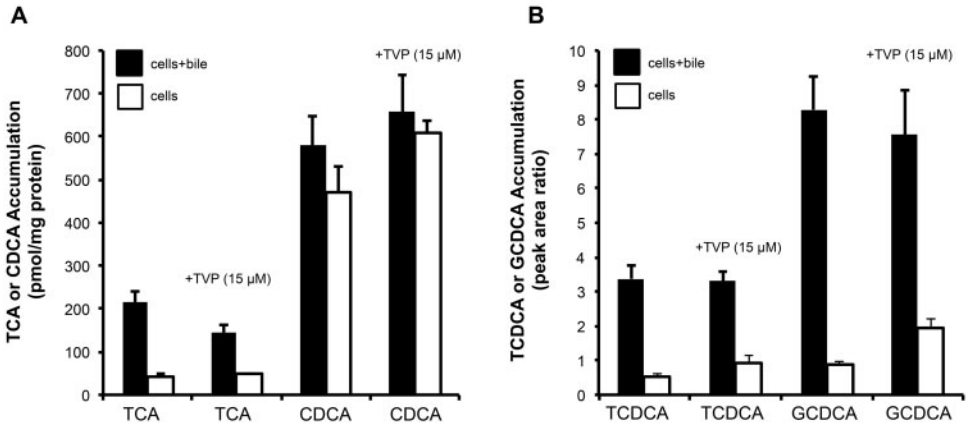

FIG. 6. Accumulation of TCA, CDCA, TCDCA, and GCDCA in the presence and absence of tolvaptan in SCHH. Accumulation of d_8-TCA (2.5 μM) and d_5-CDCA (2.5 μM) (A), or TCDCA (2.5 μM) and GCDCA (2.5 μM) (B) in cells + bile (black bars) and cells (white bars) was measured after incubating SCHH with designated bile acids in the presence or absence of tolvaptan (15 μM) for 10 min at 37°C; each value represents the mean ± SD from $n = 1$ liver in triplicate.

(<30 ml/min) than in patients with preserved renal function (Shoaf *et al.*, 2014). Thus, prolonged renal impairment may alter excretory mechanisms thereby placing a larger burden on the liver. With renal impairment in this population, an increase in systemic exposure does occur compared with non-ADPKD patients, although the differences are minimal since patients with severe renal impairment were excluded from the pivotal clinical trial (Torres *et al.*, 2012). It is worth noting, however, that the liver is the primary elimination pathway for tolvaptan/metabolites (metabolism and fecal excretion) and not urinary excretion (Shoaf *et al.*, 2012a). Hence, increasing the hepatic burden could alter hepatic exposure to tolvaptan/metabolites and may be associated with bile acid transporter inhibition, as shown in the present experiments.

BSEP inhibition has been implicated as one mechanism of DILI, although inhibition of other efflux transporters such as MRP2 and MRP4 also have been shown to exhibit an association with DILI (Köck *et al.*, 2014; Mennone *et al.*, 2006; Morgan *et al.*, 2013). Under normal physiological conditions in humans, bile acids, primarily the conjugated bile acids taurodeoxycholic acid (TDCA), glycodeoxycholic acid (GDCA), TCDCA, and GCDCA, are transported across the canalicular membrane into bile and stored in the gallbladder until released into the duodenum (Hofmann and Hagey, 2008; Rodrigues *et al.*, 2014). Bile acids concentrate in the bile ducts relative to hepatocytes; active canalicular transport via BSEP is the rate-limiting step in bile acid transport and an important determinant of bile flow (Kullak-Ublick *et al.*, 2004; Meier and Stieger, 2002). Inhibition of BSEP may lead to accumulation of bile acids within hepatocytes and subsequently induce cytotoxicity.

Cholestatic DILI is a subset of liver disease that can result from direct damage to hepatic parenchyma (eg, hepatocytes, bile ducts) through toxic or immunogenic mechanisms, and/or by impairment of biliary excretory function. Apart from genetic defects (eg, progressive familial intrahepatic cholestasis type 2), numerous drugs have been implicated in cholestasis (Padda *et al.*, 2011). Cyclosporine, a prototypical drug that can induce cholestatic liver injury, alters bile acid transport function, intrahepatic vesicle transport, canalicular membrane fluidity, and bile-acid independent bile flow (Böhme *et al.*, 1994; Bramow *et al.*, 2001; Román *et al.*, 2003; Yasumiba *et al.*, 2001). No cases of hepatotoxicity were reported during the development of troglitazone. However, this thiazolidinedione was removed from the market due to idiosyncratic liver injury. Subsequent studies, after market withdrawal, revealed that troglitazone and the sulfate conjugate of troglitazone inhibit BSEP. Further, studies with troglitazone revealed that cholestasis was more prevalent in male rats presumably due to sex-dependent differences in the toxic sulfate-conjugated species (Funk *et al.*, 2001; Kostrubsky *et al.*, 2001). These examples highlight the potential multimechanistic nature of DILI as well as the interplay between the formation and excretion of drug metabolites.

These present experiments were designed to test the hypothesis that bile acid transporter interference could be a biologically plausible mechanism to explain DILI in tolvaptan-treated patients with ADPKD. As shown, DM-4103 was a ~7.5-fold and a ~29-fold more potent inhibitor of BSEP (IC_{50}: 4.15 μM) compared with tolvaptan and DM-4107, respectively, based on IC_{50} data (Table 1). The ratio between the concentration at steady state (C_{ss}) or maximal plasma concentration (C_{max}) and the inhibitory potency (IC_{50}) is used commonly to understand the relationship between drug or metabolite exposure and inhibition (Morgan *et al.*, 2013; Zhang, 2012). According to FDA guidance, when the estimated $[I]/K_i$ or $[I]/IC_{50}$ ratio is >0.1, where $[I]$ represents the total (bound plus unbound) mean steady-state C_{max} after administration of the highest proposed clinical dose, an *in vivo* drug interaction study may be warranted (Huang *et al.*, 2008). For BSEP, both tolvaptan and DM-4107 exhibited (total) C_{max}/IC_{50} values <0.1 while DM-4103 exhibited a value of 3.78 (Table 1), which suggests that DM-4103 may be a relevant inhibitor of BSEP at the therapeutic dose of 90 mg tolvaptan. However, cellular rather than plasma concentrations of tolvaptan, DM-4103 and DM-4107 would be more relevant for predictions of efflux inhibition.

To further understand BSEP inhibition, the mechanism of inhibition was interrogated for tolvaptan and DM-4103. Inhibition of BSEP by tolvaptan was best described by a noncompetitive inhibition model ($K_i = 34.2$ μM) while DM-4103 was best described by a competitive inhibition model ($K_i = 3.77$ μM). Unlike competitive inhibition, noncompetitive inhibition reduces the rate of transport (eg, of bile acids) and the resulting effects of depressed bile acid transport may lead to accumulation of bile acids, impaired bile flow, and hepatotoxicity. This principle is supported by Woodhead *et al.* (2014) who showed that in a simulated patient population treated with CP-724,714, an anti-cancer agent terminated from further development due to hepatotoxicity thought to be due, in part, to BSEP inhibition (Guo *et al.*, 2008), clinically relevant ALT elevations developed

more frequently when BSEP inhibition was noncompetitive in nature. Mitochondrial toxicity also was implicated as a mechanism of CP-724,714 toxicity (Feng *et al.*, 2013) and clinical findings suggest that CP-724,714 exerted both hepatocellular and hepatobiliary cholestatic injury (Guo *et al.*, 2008; Munster *et al.*, 2007).

As noted earlier, inhibition of BSEP alone cannot always predict or explain DILI. This may be due, in part, to the adaptive abilities of the liver. When bile acids accumulate in hepatocytes, compensatory or salvage pathways are transcriptionally upregulated/downregulated that function as hepatoprotective mechanisms (Wagner and Trauner, 2005). MRP4, a sinusoidal bile acid efflux transporter, is normally expressed at low levels in human hepatocytes but protein expression can be increased significantly during cholestasis (Chai *et al.*, 2012; Teng and Piquette-Miller, 2007, Wagner *et al.*, 2009; Zollner *et al.*, 2006). Alterations in other bile acid efflux transporter expression/function have been reported and include MRP2, MRP3 and organic solute transporters (OSTα/OSTβ), indicating a complex adaptive response to cholestasis and/or bile acid-mediated toxicity (Boyer *et al.*, 2006; Trauner *et al.*, 1997; Zollner *et al.*, 2001). Because of these potential adaptive responses, Morgan *et al.* (2013) developed decision criteria for bile acid transporter-mediated hazard identification, which includes evaluating the inhibition of important bile acid efflux transporters (ie, MRP2, MRP3, and MRP4) in addition to BSEP. All evaluated compounds that exhibited a BSEP C_{ss}/IC_{50} ratio $\geq$0.1 and either a MRP2, MRP3, or MRP4 C_{ss}/IC_{50} ratio $\geq$0.1 were associated with some form of liver injury. These findings highlight the potential importance of compensatory mechanisms of bile acid transport when BSEP is impaired. Because inhibition of MRP-mediated transport function, in addition to BSEP, is associated with DILI, we sought to determine the inhibitory potency of tolvaptan, DM-4103, and DM-4107 on MRP2-, MRP3-, and MRP4-mediated transport function.

As shown, tolvaptan and DM-4107 showed no or marginal MRP2 inhibition, respectively (Figs. 4A–C). Although DM-4103 inhibited MRP2-mediated transport by >50% at the highest tested concentration, caution should be exercised when interpreting the IC_{50} of DM-4103 (~51.0 μM) because limits of solubility precluded testing the effects of higher tolvaptan concentrations on MRP2-mediated transport. Such was the case with DM-4103 on MRP3-mediated transport. Tolvaptan showed no effect on MRP3-mediated transport and although the IC_{50} for DM-4107 was estimated to be 61.2 μM, the C_{max}/IC_{50} value was 0.04, indicating that DM-4107 may not be a relevant inhibitor of MRP3 (Table 1). In contrast, the C_{max}/IC_{50} value for DM-4103 was 0.35 for MRP3-mediated transport. DM-4103 was an ~9-fold more potent inhibitor of MRP4-mediated transport based on IC_{50} when compared with DM-4107 (IC_{50} of 4.26 vs 37.9 μM, respectively), while tolvaptan exhibited minimal inhibition of MRP4-mediated transport (Figs. 4G–I). When taking into account plasma concentrations, DM-4103 exhibited a C_{max}/IC_{50} value of 3.69 for MRP4 (Table 1), indicating that DM-4103 may be a relevant inhibitor of the basolateral efflux transporter MRP4 since this ratio was >0.1. The effects of tolvaptan on BSEP, MRP2, and MRP4 transport were similar to the IC_{50} values reported by Morgan *et al.* (2013) (9.99, > 133, and >133 μM, respectively).

Although over-expressing cell lines and inside-out membrane vesicles are used commonly to screen for interactions at the transporter level, such systems may not be entirely predictive of the interactions that may or may not occur in complex cellular systems (eg, hepatocytes) or *in vivo* (Byrne *et al.*, 2002; Colombo *et al.*, 2013; Xia *et al.*, 2007). SCHH are a promising tool to study drug disposition and hepatotoxicity (Marion *et al.*, 2007; Swift *et al.*, 2010). Therefore, to further explore the interaction of tolvaptan with hepatocellular bile acid transporters, the disposition of tolvaptan and bile acids was evaluated in SCHH. Tolvaptan accumulation in SCHH was rapid and appeared to consist of both passive and active uptake processes (Figure 5). After a 10-min incubation with 15 μM tolvaptan, the total cellular concentration was ~500 μM, assuming that all tolvaptan was localized intracellularly. In SCHH, ~30% of the tolvaptan dose was metabolized over 10 min, with ~1% and 10% representing DM-4103 and DM-4107, respectively. The cellular concentrations of DM-4103 and DM-4107 after a 10-min incubation with 15 μM tolvaptan were ~1.71 and ~35.6 μM, respectively. Although DM-4107 is formed preferentially compared with DM-4103 in about a 10:1 ratio (DM-4107:DM4103) after 10 min in SCHH, DM-4103 is the main circulating metabolite *in vivo* (Sorbera *et al.*, 2002; Tammara *et al.*, 1999). This apparent discrepancy may be due to differences in metabolite formation rates, ie, DM-4103 and DM-4107 are downstream metabolites of tolvaptan (Tammara *et al.*, 1999).

Four bile acids (TCA, CDCA, TCDCA, and GCDCA) were used as probes to determine the inhibitory potential of tolvaptan on hepatocellular bile acid transport in SCHH. CDCA, TCDCA, and GCDCA are among the most common circulating bile acids in humans and alterations in their disposition have been implicated in cholestatic liver injury (Greim *et al.*, 1973; Ijare *et al.*, 2009; Perwaiz *et al.*, 2001; Roda *et al.*, 1998; Tagliacozzi *et al.*, 2003). Both the BEI and $Cl_{biliary}$ of TCA and CDCA in human SCHH appeared to decrease (16% and 43% compared to control, respectively, for TCA and 61% and 55% compared to control, respectively, for CDCA) when incubated with tolvaptan (Table 3). The cellular accumulation of TCA was not altered by tolvaptan, indicating that cellular basolateral efflux may be able to compensate for TCA accumulation even though TCA $Cl_{biliary}$ was decreased; TCA $Cl_{biliary}$ is ~3-fold greater than basolateral clearance in SCHH (Yang *et al.*, 2015). Similarly, both the BEI and $Cl_{biliary}$ of CDCA in SCHH were modestly decreased (Table 3). Unlike TCA, CDCA appeared to accumulate intracellularly when co-incubated with tolvaptan (increased by 1.3-fold relative to control) (Figure 6A). The cellular accumulation of TCDCA and GCDCA also appeared to increase when co-incubated with tolvaptan (increased by 1.68 - and 2.16-fold relative to control, respectively), which indicates the potential for these bile acids to accumulate, possibly due to inhibition of biliary and/or basolateral efflux (Figure 6B). The BEI for TCDCA and GCDCA also appeared to be lower when co-incubated with tolvaptan (Table 3). Inhibition of bile acid transport in SCHH is consistent with the observations from the membrane vesicle studies. These data support the hypothesis that accumulation of tolvaptan in hepatocytes may play a role in the mechanism(s) of DILI.

Although the cellular accumulation of bile acids such as TCDCA has been shown to experimentally induce liver injury *in vivo* (Sokol *et al.*, 1998), the biological importance of such changes in bile acid biliary clearance and hepatocyte accumulation in humans is not well defined. In sandwich-cultured hepatocytes, Marion *et al.* (2007) and Griffin *et al.* (2013) demonstrated that some hepatotoxic drugs were associated with impaired bile acid biliary clearance and/or increased cellular accumulation of bile acids and subsequent toxicity, similar to the present findings. Furthermore, this study examined bile acid disposition in short-term incubations, which may be exacerbated in long-term exposures as shown by the delayed presentation of bile acid-mediated toxicity of troglitazone (Yang *et al.*, 2014).

As described earlier, inhibition of hepatic bile acid transporters may not be the sole mechanism of DILI noted in the ADPKD population. Alternative mechanisms of hepatotoxicity currently are being explored. Wu *et al.* (2015) recently demonstrated that tolvaptan induces *in vitro* cellular apoptosis in HepG2 cells, potentially through several mechanisms including mitochondrial dysfunction. However, considering clinically relevant concentrations of tolvaptan and the fact that hepatotoxicity has not been reported in non-ADPKD populations, the clinical relevance of these studies remains uncertain. In addition to direct drug-induced mitochondrial dysfunction and oxidative stress, bile acids can cause hepatocellular damage by inducing swelling and abnormal mitochondrial cristae, disruption of cellular membranes, and generation of reactive oxygen species (Billington *et al.*, 1980; Philips *et al.*, 1987; Sokol *et al.*, 1993). As described by Watkins *et al.* (2015), the signature pattern of hepatic events occurred after ~3–4 months of treatment, and resolved over a prolonged period of time following discontinuation of tolvaptan. The signature pattern of hepatotoxicity suggested an adaptive immune-mediated hepatic event, which continues to be explored in patients. However, multiple mechanisms of DILI cannot be ruled out including the inhibition of bile acid transport, as shown here, and mitochondrial toxicity (Feng *et al.*, 2013). The results of studies focused on these alternative mechanism(s) will be reported subsequently. As noted at the outset of this article, the purpose of the current investigation was to test the hypothesis that inhibition of human hepatic bile acid transporters by tolvaptan and metabolites could play a role in tolvaptan-associated DILI.

It has been suggested that inhibition of NTCP-mediated bile acid uptake may provide some cellular protection from hepatic accumulation of bile acids, such as shown with bosentan (Leslie *et al.*, 2007). However, the NTCP IC_{50} value for tolvaptan (~41.5 μM) was >2-fold higher than the dose concentration in the SCHH studies, indicating that tolvaptan would have little impact on TCA uptake in hepatocytes; this is consistent with the data obtained in SCHH (Figure 6A). DM-4103 and DM-4107 concentrations in the media were negligible after a 10-min incubation (data not shown); these metabolites likely had little impact on TCA uptake in the present study. Based on C_{max} concentrations achieved with therapeutic doses of tolvaptan, only DM-4103 exhibited an I/IC_{50} >0.1 for NTCP (Table 1). However, when taking into account the unbound fraction (assuming f_u ~1%, similar to that of tolvaptan, Shoaf *et al.*, 2014), an interaction at the level of NTCP would not be expected. Tolvaptan did not appear to be a substrate of NTCP (Table 2). While NTCP is considered the primary hepatic bile acid transporter in humans, OATPs also transport endogenous anions including bile acids and bilirubin (Cui *et al.*, 2001; Meier *et al.*, 1997; Tamai *et al.*, 2000). Although inhibition of OATPs is a concern for the interaction of concomitantly administered drugs (Zhang, 2012), inhibition of OATPs has not been associated with DILI and thus, may not be relevant to understanding bile acid-mediated toxicity/disposition. Furthermore, OATP drug-drug interactions with tolvaptan have not been reported in humans (Bhatt *et al.*, 2014).

In conclusion, results of this study demonstrate that tolvaptan and metabolites inhibited multiple human hepatic proteins involved in bile acid transport (ie, NTCP, BSEP, MRP2, MRP3, and MRP4). Impaired bile acid transport by tolvaptan and/or its metabolites may negatively impact bile acid homeostasis, which may explain, in part, the mechanism(s) behind liver injury in tolvaptan-treated ADPKD patients. However, the fact that liver injury has been observed only in patients with ADPKD, and that no evidence of cholestasis (ie, no clinically significant increases in alkaline phosphatase) was observed in the ADPKD clinical trial (Torres *et al.*, 2012), suggests that other mechanisms may predispose this patient population to DILI. Research into other genetic and nongenetic mechanisms of tolvaptan-induced DILI is on-going.

FUNDING

Funding was provided by Otsuka Pharmaceutical Development and Commercialization, Inc., and, in part, by the National Institute of General Medical Sciences of the National Institutes of Health (NIH) under Award Number R01GM041935 (K.L.R.B.). The content is solely the responsibility of the authors and does not necessarily represent the official views of Otsuka or the NIH.

ACKNOWLEDGMENTS

We thank Kevin Le and Izna Ali for technical assistance with membrane vesicle studies, and Cassandra Hubert for assistance with the LC-MS/MS analysis of TCA and CDCA. Drs. M. Pan and W.J. Brock are employees of Otsuka Pharmaceutical Development and Commercialization, Inc. Dr. K.R. Brouwer, Ms. K.M. Freeman, and Dr. R.L. St. Claire are employed by Qualyst Transporter Solutions, LLC. Dr. K.L.R. Brouwer is a co-inventor of the sandwich-cultured hepatocyte technology for quantification of biliary excretion (B-CLEAR®) and related technologies, which have been licensed exclusively to Qualyst Transporter Solutions, LLC. This work was presented, in part, at the 2015 Society of Toxicology, San Diego, CA (posters 517 and 570), and the 2015 American Association of Pharmaceutical Scientists-International Transporter Consortium Workshop on Drug Transporters in ADME, Baltimore, MD (poster M1031).

REFERENCES

Akaike, H. (1974). A new look at the statistical model identification. *IEEE Trans. Auto. Control* **AC-19**, 716–723.

Akita, H., Suzuki, H., Hirohashi, T., Takikawa, H., and Sugiyama, Y. (2002). Transport activity of human MRP3 expressed in Sf9 cells: comparative studies with rat MRP3. *Pharm. Res.* **19**, 34–41.

Bhatt, P. R., McNeely, E. B., Lin, T. E., Adams, K. F., and Patterson, J. H. (2014). Review of tolvaptan's pharmacokinetic and pharmacodynamic properties and drug interactions. *J. Clin. Med.* **3**, 1276–1290.

Billington, D., Evans, C. E., Godfrey, P. P., and Coleman, R. (1980). Effects of bile salts on the plasma membranes of isolated rat hepatocytes. *Biochem. J.* **188**, 321–327.

Boertien, W. E., Meijer, E., de Jong P. E., ter Horst, G. J., Renken, R. J., van der Jagt, E. J., Kappert, P., Ouyang, J., Engels, G. E., van Oeveren, W., *et al.* (2015). Short-term effects of tolvaptan in individuals with autosomal dominant polycystic kidney disease at various levels of kidney function. *Am. J. Kidney Dis.* **65**, 833–841.

Boyer, J. L., Trauner, M., Mennone, A., Soroka, C. J., Cai, S. Y., Moustafa, T., Zollner, G., Lee, J. Y., and Ballatori, N. (2006). Upregulation of a basolateral FXR-dependent bile acid efflux transporter OSTalpha-OSTbeta in cholestasis in humans and rodents. *Am. J. Physiol. Gastrointest. Liver Physiol.* **290**, G1124–G1130.

Böhme, M., Müller, M., Leier, I., Jedlitschky, G., and Keppler, D. (1994). Cholestasis caused by inhibition of the adenosine triphosphate-dependent bile salt transport in rat liver. *Gastroenterology* **107**, 255–265.

Bramow, S., Ott, P., Thomsen Nielsen, F., Bangert, K., Tygstrup, N., and Dalhoff, K. (2001). Cholestasis and regulation of genes related to drug metabolism and biliary transport in rat liver following treatment with cyclosporine A and sirolimus (Rapamycin). *Pharmacol. Toxicol.* **89**, 133–139.

Byrne, J. A., Strautnieks, S. S., Mieli-Vergani, G., Higgins, C. F., Linton, K. J., and Thompson, R. J. (2002). The human bile salt export pump: characterization of substrate specificity and identification of inhibitors. *Gastroenterology* **123**, 1649–1658.

Chai, J., He, Y., Cai, S. Y., Jiang, Z., Wang, H., Li, Q., Chen, L., Peng, Z., He, X., Wu, X., *et al.* (2012). Elevated hepatic multidrug resistance-associated protein 3/ATP-binding cassette subfamily C 3 expression in human obstructive cholestasis is mediated through tumor necrosis factor alpha and c-Jun NH2-terminal kinase/stress-activated protein kinase-signaling pathway. *Hepatology* **55**, 1485–1494.

Colombo, F., Poirier, H., Rioux, N., Montecillo, M. A., Duan, J., and Ribadeneira, M. D. (2013). A membrane vesicle-based assay to enable prediction of human biliary excretion. *Xenobiotica* **43**, 915–919.

Cui, Y., König, J., Leier, I., Buchholz, U., and Keppler, D. (2001) Hepatic uptake of bilirubin and its conjugates by the human organic anion transporter SLC21A6. *J. Biol. Chem.* **276**, 9626–9630.

Feng, B., Xu, J. J., Bi, Y. A., Mireles, R., Davidson, R., Duignan, D. B., Campbell, S., Kostrubsky, V. E., Dunn, M. C., Smith, A. R., *et al.* (2013). Role of hepatic transporters in the disposition and hepatotoxicity of a HER2 tyrosine kinase inhibitor CP-724,714. *Toxicol. Sci.* **108**, 492–500.

Fukunami, M., Matsuzaki, M., Hori, M., Izumi, T., and Tolvaptan Investigators. (2011). Efficacy and safety of tolvaptan in heart failure patients with sustained volume overload despite the use of conventional diuretics: a phase III open-label study. *Cardiovasc. Drugs Ther.* **25**, S47–S56.

Funk, C., Pantze, M., Jehle, L., Ponelle, C., Scheuermann, G., Lazendic, M., and Gasser, R. (2001). Troglitazone-induced intrahepatic cholestasis by an interference with the hepatobiliary export of bile acids in male and female rats. Correlation with the gender difference in troglitazone sulfate formation and the inhibition of the canalicular bile salt export pump (BSEP) by troglitazone and troglitazone sulfate. *Toxicology* **167**, 83–98.

Ghibellini, G., Vasist, L. S., Leslie, E. M., Heizer, W. D., Kowalsky, R. J., Calvo, B. F., and Brouwer, K. L. (2007). In vitro-in vivo correlation of hepatobiliary drug clearance in humans. *Clin. Pharmacol. Ther.* **81**, 406–413.

Greim, H., Czygan, P., Schaffner, F., and Popper, H. (1973). Determination of bile acids in needle biopsies of human liver. *Biochem. Med.* **8**, 280–286.

Griffin, L. M., Watkins, P. B., Perry, C. H., St Claire, R. L. 3rd, and Brouwer, K. L. (2013). Combination lopinavir and ritonavir alter exogenous and endogenous bile acid disposition in sandwich-cultured rat hepatocytes. *Drug Metab. Dispos.* **41**, 188–196.

Guo, F., Letrent, S. P., Munster, P. N., Britten, C. D., Gelmon, K., Tolcher, A. W., and Sharma, A. (2008). Pharmacokinetics of a HER2 tyrosine kinase inhibitor CP-724,714 in patients with advanced malignant HER2 positive solid tumors: correlations with clinical characteristics and safety. *Cancer Chemother. Pharmacol.* **62**, 97–109.

Higashihara, E., Torres, V. E., Chapman, A. B., Grantham, J. J., Bae, K., Watnick, T. J., Horie, S., Nutahara, K., Ouyang, J., Krasa, H. B., *et al.* (2011). TEMPO Formula and 156-05-002 study investigators. Tolvaptan in autosomal dominant polycystic kidney disease: three years' experience. *Clin. J. Am. Soc. Nephrol.* **6**, 2499–2507.

Hofmann, A. F., and Hagey, L. R. (2008). Bile acids: chemistry, pathochemistry, biology, pathobiology, and therapeutics. *Cell Mol. Life Sci.* **65**, 2461–2483.

Huang, S. M., Strong, J. M., Zhang, L., Reynolds, K. S., Nallani, S., Temple, R., Abraham, S., Habet, S. A., Baweja, R. K., Burckart, G. J., *et al.* (2008). New era in drug interaction evaluation: US Food and Drug Administration update on CYP enzymes, transporters, and the guidance process. *J. Clin. Pharmacol.* **48**, 662–670.

Ijare, O. B., Bezabeh, T., Albiin, N., Arnelo, U., Bergquist, A., Lindberg, B., and Smith, I. C. (2009). Absence of glycochenodeoxycholic acid (GCDCA) in human bile is an indication of cholestasis: a 1H MRS study. Absence of glycochenodeoxycholic acid (GCDCA) in human bile is an indication of cholestasis: a 1H MRS study. *NMR Biomed.* **22**, 471–479.

Kim, S. R., Hasunuma, T., Sato, O., Okada, T., Kondo, M., and Azuma, J. (2011). Pharmacokinetics, pharmacodynamics and safety of tolvaptan, a novel, oral, selective nonpeptide AVP V2-receptor antagonist: results of single- and multiple-dose studies in healthy Japanese male volunteers. *Cardiovasc. Drugs Ther.* **25**, S5–S17.

Köck, K., Ferslew, B. C., Netterberg, I., Yang, K., Urban, T. J., Swaan, P. W., Stewart, P. W., and Brouwer, K. L. (2014). Risk factors for development of cholestatic drug-induced liver injury: inhibition of hepatic basolateral bile acid transporters multidrug resistance-associated proteins 3 and 4. *Drug Metab. Dispos.* **42**, 665–674.

Kostrubsky, V. E., Vore, M., Kindt, E., Burliegh, J., Rogers, K., Peter, G., Altrogge, D., and Sinz, M. W. (2001). The effect of troglitazone biliary excretion on metabolite distribution and cholestasis in transporter-deficient rats. *Drug Metab. Dispos.* **29**, 1561–1566.

Kullak-Ublick, G. A., Stieger, B., and Meier, P. J. (2004). Enterohepatic bile salt transporters in normal physiology and liver disease. *Gastroenterology* **126**, 322–342.

Leslie, E. M., Watkins, P. B., Kim, R. B., and Brouwer, K. L. (2007). Differential inhibition of rat and human Na+-dependent taurocholate cotransporting polypeptide (NTCP/SLC10A1) by bosentan: a mechanism for species differences in hepatotoxicity. *J. Pharmacol. Exp. Ther.* **321**, 1170–1178.

Liu, X., LeCluyse, E. L., Brouwer, K. R., Gan, L. S., Lemasters, J. J., Stieger, B., Meier, P. J., and Brouwer, K. L. (1999a). Biliary excretion in primary rat hepatocytes cultured in a collagen-sandwich configuration. *Am. J. Physiol.* **277**, G12–G21.

Liu, X., Chism, J. P., LeCluyse, E. L., Brouwer, K. R., and Brouwer, K. L. (1999b). Correlation of biliary excretion in sandwich-culture rat hepatocytes and in vivo in rats, *Drug Metab. Dispos.* **27**, 637–644.

Marion, T. L., Leslie, E. M., and Brouwer, K. L. (2007). Use of sandwich-cultured hepatocytes to evaluate impaired bile acid transport as a mechanism of drug-induced hepatotoxicity. *Mol. Pharm.* **4**, 911–918.

Marion, T. L., Perry, C. H., St Claire, R. L., 3rd, and Brouwer, K. L. (2012). Endogenous bile acid disposition in rat and human sandwich-cultured hepatocytes. *Toxicol. Appl. Pharmacol.* **261**, 1–9.

Meier, P. J., and Stieger, B. (2002). Bile salt transporters. *Annu. Rev. Physiol.* **64**, 635–661.

Meier, P. J., Eckhardt, U., Schroeder, A., Hagenbuch, B., and Stieger, B. (1997). Substrate specificity of sinusoidal bile acid and organic anion uptake systems in rat and human liver. *Hepatology* **26**, 1667–1677.

Mennone, A., Soroka, C. J., Cai, S. Y., Harry, K., Adachi, M., Hagey, L., Schuetz, J. D., and Boyer, J. L. (2006). $Mrp4^{-/-}$ mice have an impaired cytoprotective response in obstructive cholestasis. *Hepatology* **43**, 1013–1021.

Morgan, R. E., Trauner, M., van Staden, C. J., Lee, P. H., Ramachandran, B., Eschenberg, M., Afshari, C. A., Qualls, C. W., Jr., Lightfoot-Dunn, R., and Hamadeh, H. K. (2010). Interference with bile salt export pump function is a susceptibility factor for human liver injury in drug development. *Toxicol. Sci.* **118**, 485–500.

Morgan, R. E., van Staden, C. J., Chen, Y., Kalyanaraman, N., Kalanzi, J., Dunn, R. T., Afshari, C. A., and Hamadeh, H. K. (2013). A multifactorial approach to hepatobiliary transporter assessment enables improved therapeutic compound development. *Toxicol. Sci.* **136**, 216–2141.

Munster, P. N., Britten, C. D., Mita, M., Gelmon, K., Minton, S. E., Moulder, S., Slamon, D. J., Guo, F., Letrent, S. P., Denis, L., *et al.* (2007). First study of the safety, tolerability, and pharmacokinetics of CP-724,714 in patients with advanced malignant solid HER2-expressing tumors. *Clin. Cancer Res.* **13**, 1238–1245.

Oi, A., Morishita, K., Awogi, T., Ozaki, A., Umezato, M., Fujita, S., Hosoki, E., Morimoto, H., Ishiharada, N., Ishiyama, H., *et al.* (2011). Nonclinical safety profile of tolvaptan. *Cardiovasc. Drugs Ther.* **1**, S91–S99.

Padda, M. S., Sanchez, M., Akhtar, A. J., and Boyer, J. L. (2011). Drug-induced cholestasis. *Hepatology* **53**, 1377–1387.

Patel, M. S., Kandula, P., Wojciechowski, D., Markmann, J. F., and Vagefi, P. A. (2014). Trends in the management and outcomes of kidney transplantation for autosomal dominant polycystic kidney disease. *J. Transplant.* **2014**, Article ID 675697.

Perez, M. J., and Briz, O. (2009). Bile-acid-induced cell injury and protection. *World J. Gastroenterol.* **15**, 1677–1689.

Perwaiz, S., Tuchweber, B., Mignault, D., Gilat, T., and Yousef, I. M. (2001). Determination of bile acids in biological fluids by liquid chromatography-electrospray tandem mass spectrometry. *J. Lipid Res.* **42**, 114–119.

Phillips, M. J., Poucell, S., Patterson, J., and Valencia, P. (1987). Cholestasis. In *The Liver: An Atlas and Text of Ultrastructural Pathology* (M. J. Phillips, S. Poucell, J. Patterson, and P. Valencia, Eds.), pp. 101–158. Raven Press, New York.

Qualyst Transporter Solutions Technical Application Bulletin TAB Biol 005. (2011). TAB Biol 005v2.

Rius, M., Hummel-Eisenbeiss, J., Hofmann, A. F., and Keppler, D. (2006). Substrate specificity of human ABCC4 (MRP4)-mediated co-transport of bile acids and reduced glutathione. *Am. J. Physiol. Gastrointest. Liver Physiol.* **290**, G640–G649.

Roda, A., Piazza, F., Baraldini, M., Speroni, E., Guerra, M. C., Cerré, C., and Cantelli Forti, G. (1998). Taurohyodeoxycholic acid protects against taurochenodeoxycholic acid-induced cholestasis in the rat. *Hepatology* **27**, 520–525.

Rodrigues, A. D., Lai, Y., Cvijic, M. E., Elkin, L. L., Zvyaga, T., and Soars, M. G. (2014). Drug-induced perturbations of the bile acid pool, cholestasis, and hepatotoxicity: mechanistic considerations beyond the direct inhibition of the bile salt export pump. *Drug Metab. Dispos.* **42**, 566–574.

Román, I. D., Fernández-Moreno, M. D., Fueyo, J. A., and Roma, M. G. (2003). Coleman R Cyclosporin A induced internalization of the bile salt export pump in isolated rat hepatocyte couplets. *Toxicol. Sci.* **71**, 276–281.

Sakaida, I. (2014). Tolvaptan for the treatment of liver cirrhosis oedema. *Expert Rev. Gastroenterol. Hepatol.* **8**, 461–470.

Schrier, R. W., Gross, P., Gheorghiade, M., Berl, T., Verbalis, J. G., Czerwiec, F. S., and Orlandi, C. (2006). SALT Investigators. Tolvaptan, a selective oral vasopressin V2-receptor antagonist, for hyponatremia. *N. Engl. J. Med.* **355**, 2099–2112.

Senior, J. R. (2014). Evolution of the Food and Drug Administration approach to liver safety assessment for new drugs: current status and challenges. *Drug Saf.* **37**(Suppl 1), S9–S17.

Shoaf, S. E., Bricmont, P., and Mallikaarjun, S. (2012a). Absolute bioavailability of tolvaptan and determination of minimally effective concentrations in healthy subjects. *Int. J. Clin. Pharmacol. Ther.* **50**, 150–156.

Shoaf, S. E., Bricmont, P., and Mallikaarjun, S. (2012b). Effects of CYP3A4 inhibition and induction on the pharmacokinetics and pharmacodynamics of tolvaptan, a non-peptide AVP antagonist in healthy subjects. *Br. J. Clin. Pharmacol.* **73**, 579–587.

Shoaf, S. E., Bricmont, P., and Mallikaarjun, S. (2014). Pharmacokinetics and pharmacodynamics of oral tolvaptan in patients with varying degrees of renal function. *Kidney Int.* **85**, 953–961.

Shoaf, S. E., Wang, Z., Bricmont, P., and Mallikaarjun, S. (2007). Pharmacokinetics, pharmacodynamics, and safety of tolvaptan, a nonpeptide AVP antagonist, during ascending single-dose studies in healthy subjects. *J. Clin. Pharmacol.* **47**, 1498–1507.

Sokol R J., Devereaux, M., Khandwala, R., and O'Brien, K. (1993). Evidence for involvement of oxygen free radicals in bile acid toxicity to isolated rat hepatocytes. *Hepatology* **17**, 869–881.

Sokol R. J., McKim, J. M., Jr., Goff, M. C., Ruyle, S. Z., Devereaux, M. W., Han, D., Packer, L., and Everson, G. (1998). Vitamin E reduces oxidant injury to mitochondria and the hepatotoxicity of taurochenodeoxycholic acid in the rat. *Gastroenterology* **114**, 164–174.

Sorbera, L. A., Castaner, J., Bayes, M., and Silvestre, J. (2002). Tolvaptan: treatment for heart failure vasopressin V_2 antagonist. *Drugs Future.* **27**, 350–357.

Swift, B., Pfeifer, N. D., and Brouwer, K. L. (2010). Sandwich-cultured hepatocytes: an in vitro model to evaluate hepatobiliary transporter-based drug interactions and hepatotoxicity. *Drug Metab. Rev.* **42**, 446–471.

Tagliacozzi, D., Mozzi, A. F., Casetta, B., Bertucci, P., Bernardini, S., Di Ilio, C., Urbani, A., and Federici, G. (2003). Quantitative analysis of bile acids in human plasma by liquid chromatography-electrospray tandem mass spectrometry: a simple and rapid one-step method. *Clin. Chem. Lab. Med.* **41**, 1633–1641.

Tamai, I., Nezu, J., Uchino, H., Sai, Y., Oku, A., Shimane, M., and Tsuji, A. (2000). Molecular identification and characterization of novel members of the human organic anion transporter (OATP) family. *Biochem. Biophys. Res. Commun.* **273**, 251–260.

Tammara, B. K., Sekar, K. S., and Brumer, S. L. (1999). The disposition of a single dose of ^{14}C OPC-41061 in healthy male volunteers. *Ann. Meeting Am. Assoc. Pharm. Sci.* Abstract 2025.

Teng, S., and Piquette-Miller, M. (2007). Hepatoprotective role of PXR activation and MRP3 in cholic acid-induced cholestasis. *Br. J. Pharmacol.* **151**, 367–376.

Torres, V. E., Chapman, A. B., Devuyst, O., Gansevoort, R. T., Grantham, J. J., Higashihara, E., Perrone, R. D., Krasa, H. B., Ouyang, J., and Czerwiec, F. S. (2012). TEMPO 3:4 trial investigators. Tolvaptan in patients with autosomal dominant polycystic kidney disease. *N. Engl. J. Med.* **367**, 2407–2418.

Torres, V. E., Harris, P. C., and Pirson, Y. (2007). Autosomal dominant polycystic kidney disease. *Lancet*. **369**, 1287–1301.

Trauner, M., Arrese, M., Soroka, C. J, Ananthanarayanan, M., Koeppel, T. A., Schlosser, S. F., Suchy, F. J., Keppler, D., and Boyer, J. L. (1997). The rat canalicular conjugate export pump (Mrp2) is down-regulated in intrahepatic and obstructive cholestasis. *Gastroenterology*. **113**, 255–64.

Wagner, M., and Trauner, M. (2005). Transcriptional regulation of hepatobiliary transport systems in health and disease: implications for a rationale approach to the treatment of intrahepatic cholestasis. *Ann. Hepatol.* **4**, 77–99.

Wagner, M., Zollner, G., and Trauner, M. (2009). New molecular insights into the mechanisms of cholestasis. *J. Hepatol.* **51**, 565–580.

Watkins, P. B., Lewis, J. H., Kaplowitz, N., Alpers, D. H., Blais, J. D., Smotzer, D. M., Krasa, H., Ouyang, J., Torres, V. E., Czerwiec, F. S., *et al.* (2015). Clinical pattern of tolvaptan-associated liver injury in subjects with autosomal dominant polycystic kidney disease: analysis of clinical trials database. *Drug Saf.* **38**, 1103–1113.

Woodhead, J. L., Yang, K., Siler, S. Q., Watkins, P. B., Brouwer, K. L., Barton, H. A., and Howell, B. A. (2014). Exploring BSEP inhibition-mediated toxicity with a mechanistic model of drug-induced liver injury. *Front. Pharmacol.* **5**, Article: 240.

Wu, Y., Beland, F. A., Chen, S., Liu, F., Guo, L., and Fang, J.-L. (2015). Mechanisms of tolvaptan-induced toxicity in HepG2 cells. *Biochem. Pharmacol.* **95**, 324–336.

Xia, C. Q., Milton, M. N., and Gan, L. S. (2007). Evaluation of drug-transporter interactions using in vitro and in vivo models. *Curr. Drug. Metab.* **8**, 341–363.

Yamamura, Y., Nakamura, S., Itoh, S., Hirano, T., Onogawa, T., Yamashita, T., Yamada, Y., Tsujimae, K., Aoyama, M., Kotosai, K., *et al.* (1998). OPC-41061, a highly potent human vasopressin V2-receptor antagonist: pharmacological profile and aquaretic effect by single and multiple oral dosing in rats. *J. Pharmacol. Exp. Ther.* **287**, 860–867.

Yang, K., Pfeifer, N. D., Kock, K., and Brouwer, K. L. (2015). Species differences in hepatobiliary disposition of taurocholic acid in human and rat sandwich-cultured hepatocytes: implications for drug-induced liver injury. *J. Pharmacol. Exp. Ther.* **353**, 415–423.

Yang, K., Woodhead, J. L., Watkins, P. B., Howell, B. A., and Brouwer, K. L. (2014). Systems pharmacology modeling predicts delayed presentation and species differences in bile acid-mediated troglitazone hepatotoxicity. *Clin. Pharmacol. Ther.* **96**, 589–598.

Yasumiba, S., Tazuma, S., Ochi, H., Chayama, K., and Kajiyama, G. (2001). Cyclosporin A reduces canalicular membrane fluidity and regulates transporter function in rats. *Biochem. J.* **354**, 591–596.

Zelcer, N., Reid, G., Wielinga, P., Kuil, A., van der Heijden, I., Schuetz, J. D., and Borst, P. (2003). Steroid and bile acid conjugates are substrates of human multidrug-resistance protein (MRP) 4 (ATP-binding cassette C4). *Biochem. J.* **71**, 361–367.

Zhang, L. (2012). *Guidance for Industry: Drug Interaction Studies – Study Design, Data Analysis, Implications for Dosing, and Labeling Recommendations*. Office of Clinical Pharmacology, Food and Drug Administration, Silver Spring, MD.

Zollner, G., Fickert, P., Zenz, R., Fuchsbichler, A., Stumptner, C., Kenner, L., Ferenci, P., Stauber, R.E., Krejs, G.J., Denk, H., *et al.* (2001). Hepatobiliary transporter expression in percutaneous liver biopsies of patients with cholestatic liver diseases. *Hepatology* **33**, 633–646.

Zollner, G., Marschall, H. U., Wagner, M., and Trauner, M. (2006). Role of nuclear receptors in the adaptive response to bile acids and cholestasis: pathogenetic and therapeutic considerations. *Mol. Pharm.* **3**, 231–251.